

SLAVKO BERNIK^{1,2}, MATEJKA PODLOGAR^{1,2}
NINA DANEU^{1,2}, ALEKSANDER REČNIK^{1,2}

Scientific paper
UDC:620.186

A novel approach to tailoring the microstructure and electrical characteristics of ZnO-based varistor ceramics via inversion-boundary (IB) induced grain growth

ZnO-based varistors with exceptional current-voltage (I-U) nonlinearity are widely used in the over-voltage protection of electrical equipment and devices at voltages ranging from a few volts to several hundred kilo-volts. Their breakdown voltage is strongly influenced by the average ZnO grain size: a coarse-grained microstructure results in a low breakdown voltage for the ceramics, while a fine-grained microstructure is required for a high breakdown voltage. The grain size in high-voltage varistor ceramics is controlled by the addition of a spinel-forming additive, typically Sb_2O_3 . The concept of grain-growth inhibition due to the reduced grain-boundary mobility caused by the pinning effect of the spinel particles largely defines the composition of the ZnO-based varistor ceramics with additions of 7 to 10 wt.% of varistor dopants to the ZnO. Spinel-forming dopants such as Sb_2O_3 , TiO_2 and SnO_2 also result in the formation of inversion boundaries (IBs) in the ZnO grains. We have identified an IB-induced grain-growth mechanism which primarily controls the microstructure development, while the role of the spinel is subordinated. This understanding enabled us to prepare varistor ceramics with excellent I-U nonlinearity and breakdown voltages, ranging from 120V/mm to 350V/mm with the amount of varistor dopants added to the ZnO reduced to only about 3 wt.%.

INTRODUCTION

Electrical transients and overvoltage protection

The most common sources of electrical transients are lightning strikes. These are unpredictable, related to the release of an extremely large amount of energy, and result in very high currents and a voltage increase. Hence, lightning strikes are the most dangerous source of electrical transients to any installation, building and equipment, and also to people in the building using that equipment. Installing a lightning conductor can prevent the effects of a direct strike into a building. However, there are number of secondary effects. The direct strike injects an extremely powerful shock current into the conductor (from a few kA to 200kA) and produces a surge voltage. The current wave travels the path of least resistance to ground and resembles a voltage source transient wave to other equipment that is impedance insulated. Such a voltage surge may be several thousand times greater than the insulating capacity of the device, not to mention their rated operating voltages. Indirect transients on overhead lines are caused by cloud-to-cloud discharges that create magnetic fields and induce voltage on the conductors. Hence, the electrical current spreads to neighbouring buildings over con

necting electrical, telephone, gas or water networks, causing damage and destruction. Over-voltage influences are, therefore, the result of ohmic, inductive and capacitive connections. In practice it has been shown that the influence of a lightning strike spreads in a radius of 1.5 km from the centre of the strike, which can be a building or in the cloud. At such a distance a major redistribution of charge can induce 70,000V on a 1000-m power cable. If the buildings are interconnected with networks then the influence on the equipment is from an even greater distance. Consequently, any line can provide a direct path to your building (AC power lines, DC communication lines, gas and water networks) and equipment through which voltage surges and electrical transients can travel and cause damage. Research suggests that realistic U.S. lightning costs and losses may exceed \$5 to \$6 billion per year.

Although the life span of the transient electrical surges is very short, the amount of energy that is carried can be extremely high. A typical transient event occurs in the nano- to milli-second time domain carrying several thousand to several tens of thousands of volts and up to a few hundred or even several tens of thousands of amps of current. Hence, transients can damage or even destroy equipment and installations, cause huge fires and endanger human lives and property. It is of essential importance in our modern, technologically highly developed, interconnected and mutually dependent society in which our working places and homes are equipped with sensitive systems

Address authors: ¹Jožef Stefan Institute, Jamova cesta 39, 1000 Ljubljana, Slovenia, ²Center of Excellence NAMASTE, Jamova cesta 39, 1000 Ljubljana, Slovenia

Paper received: 21. 03. 2011.

and equipment (telecommunications, PCs and PCs peripherals, audio-video equipment, home appliances, etc.) to ensure their undisturbed operation. An estimated 24,000 people are killed by direct lightning strikes around the world each year and about 240,000 are injured. While these losses of lives can be reduced only by people's awareness of lightning danger and appropriate behaviour in the time of thunderstorms, the installation of a properly planned protection system can effectively prevent costs due to property damage and destruction, the loss and expense of valuable production time and contributes to a higher quality and safety of human lives at the workplace and in homes. Surge protection devices (SPDs) are used for the protection of power and telecommunication lines, buildings and their electrical installations, equipment, devices and personnel against transient electrical surges [1,2]. Metal oxide varistors (MOVs) are often used as the active core of the SPDs.

ZnO-based varistor ceramics

Zinc oxide (ZnO) varistors are ceramic devices with highly nonlinear current-voltage (I-U) characteristics, commonly expressed as $I = KU^\alpha$ (K-constant, α -nonlinear coefficient), and high current- and energy-absorption capabilities.

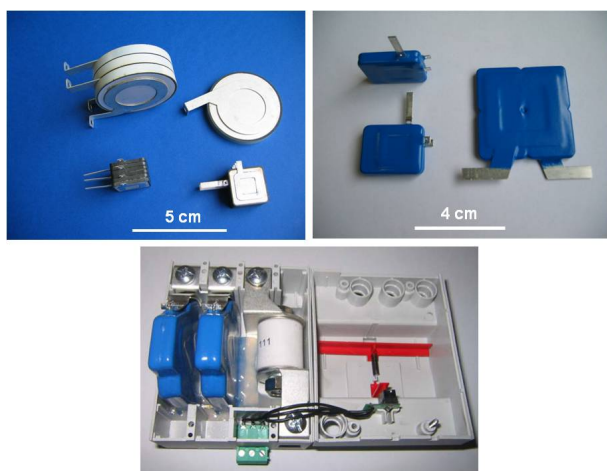


Fig. 1: Varistors, varistor stacks (top images) and varistor-based SPDs (bottom image).

The nonlinear coefficient α indicates the degree of non-ohmic property and typically has values between 20 and 70. Because of these unique and superior physical properties combined with cost-effective production, ZnO varistors (Fig. 1) are widely used in a broad range of voltages from a few volts to several 100 kilovolts for the protection of electronic components and circuits against voltage surges and as the valve elements of arresters (Fig. 2) for the voltage stabilisation of power lines. When the device under protection is subject to a transient overvoltage, the varistor in parallel to it is immediately active and

switches in a matter of nano-seconds from a highly resistive to a highly conductive state; it forms a preferential route for the flow of the disturbance energy to earth, and prevents a rise in the transient voltage and damage to the equipment [3-5].

The I-U non-linear characteristic of the ZnO varistor is a phenomenon of the grain boundaries between semiconducting ZnO grains. The voltage across the non-ohmic grain boundary is ideally about 3.2 V at breakdown [6,7]. The breakdown voltage of varistor ceramics is directly proportional to the number of grain boundaries per unit of thickness and therefore to the inverse of the ZnO grain size. The breakdown voltage of the varistor can be controlled by the thickness of the varistor and through the microstructure (i.e. ZnO grain size) of the ceramic body. For high-voltage applications fine-grained varistor ceramics are required and for low-voltage applications a coarser-grained microstructure is preferred. While at low currents, in the pre-breakdown region, the electrical characteristics of the varistor ceramics are determined by the resistivity of the grain boundaries, at high currents, in the upturn region of the I-U characteristics, a high conductivity of the ZnO grains is required.

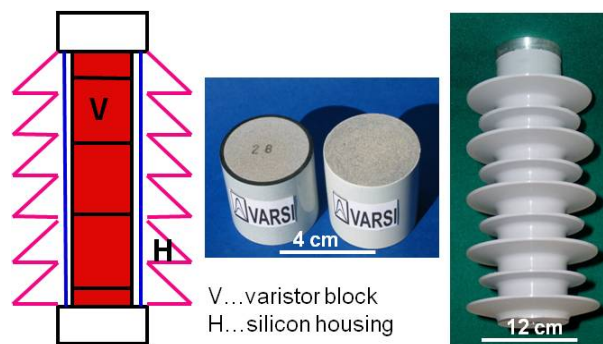


Fig. 2: Schematic presentation of arrester (left), typical varistor blocks (middle) used in arresters and 24-kV arrester (right).

ZnO-based varistor ceramics are obtained by the addition of about 7 to 10 wt. % of oxides of Bi, Sb, Ti, Co, Mn, Ni, Cr, Al and others to ZnO powder, followed by sintering in air. Each of the dopants have a distinctive role in forming the electrical characteristics of the varistor ceramics. The Bi_2O_3 is the basic dopant, which creates the nonohmic behavior of ZnO-based varistor ceramics by forming the electrostatic barriers at the grain boundaries. Other dopants are added to enhance the nonlinear characteristics and control the microstructure development. During the firing process, which usually takes place at a temperature between 1100° and 1300°C , dopants react with the ZnO and the microstructure of the

varistor is formed in the presence of a Bi_2O_3 -rich liquid phase. The typical microstructure of varistor ceramics is rather complex (Fig. 3), composed of the matrix of the ZnO grains with Bi-rich secondary phases and $\text{Zn}_7\text{Sb}_2\text{O}_{12}$ spinel along the grain boundaries and at the triple junctions. Depending on the starting composition and the heat-treatment regime the $\text{Bi}_3\text{Zn}_2\text{Sb}_3\text{O}_{14}$ pyrochlore-type phase can be present as well. The ZnO grains incorporate cobalt, manganese and nickel, which enhance their conductivity. These varistor dopants also incorporate in significant amounts into the spinel phase. The spinel phase is generally considered to inhibit the growth of the ZnO grains; therefore, Sb_2O_3 is commonly added to high-voltage varistor ceramics. The spinel phase can be formed either by the reaction of Sb_2O_3 with ZnO and/or via a $\text{Sb}_3\text{ZnBi}_3\text{O}_{14}$ pyrochlore phase. The pyrochlore phase in the reaction with the ZnO phase decomposes into the spinel phase and a Bi_2O_3 -rich liquid phase at temperatures above 900°C . The microstructure development is therefore strongly influenced by the Sb/Bi ratio, which affects the temperature of formation of the liquid phase. At the $\text{Sb/Bi} < 1$ the liquid phase forms already at 740°C by the melting of the eutectic in the system ZnO– Bi_2O_3 . When $\text{Sb/Bi} > 1$, all the Bi_2O_3 is bound into the pyrochlore phase and the liquid phase appears only after the decomposition of the pyrochlore phase at a higher temperature [8-10].

As the threshold voltage (breakdown voltage per unit thickness; V/cm) of the varistor ceramics is proportional to the ZnO grain size, control of the grain growth in the processing of varistor ceramics is essential for the successful application of varistors in over-voltage protection in a broad range from a few volts up to several kilovolts. The production of varistor ceramics with varying breakdown voltages per unit thickness – low, medium or high – makes it possible to produce varistors with suitable dimensions (thickness) for any required voltage. Hence, microstructure development and grain growth in ZnO ceramics have been intensively studied in the past and the main emphasis was given to those varistor dopants that significantly influence the grain growth: Bi_2O_3 , which not only induces the non-linearity in ZnO ceramics but also introduces a liquid phase to the system [11-13], and spinel-forming dopants, especially Sb_2O_3 [14-16], TiO_2 [17,18] and Al_2O_3 [19-22], which are added to control the ZnO grain size in varistor ceramics. While Sb_2O_3 is a standard dopant in fine-grained high-voltage varistor ceramics, TiO_2 is added to coarse-grained varistor ceramics with a low breakdown voltage.

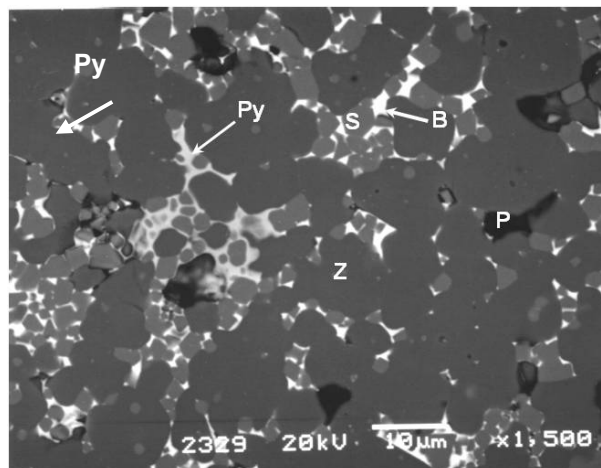


Fig. 3: Backscattered-electron (BE) image from scanning electron microscope (SEM) of a typical microstructure of a nowadays standard varistor ceramic with the addition of 7 to 10 wt.% of varistor dopants to ZnO. Z: ZnO; B: Bi_2O_3 -rich phase; Py: $\text{Bi}_3\text{Zn}_2\text{Sb}_3\text{O}_{14}$ pyrochlore phase; S: $\text{Zn}_7\text{Sb}_2\text{O}_{12}$ spinel phase; P: pore.

The inhibition of the grain growth in Sb_2O_3 -doped [14-16] and also Al_2O_3 -doped [19-21] samples is generally explained by the reduced mobility of the ZnO grain boundaries due to the pinning effect of the spinel grains at the ZnO grain boundaries. A microstructure similar to that of Sb_2O_3 is obtained with SnO_2 -doped varistor ceramics [23]. Sb_2O_3 , SnO_2 and TiO_2 form a spinel phase with ZnO, and they also trigger the formation of inversion boundaries (IBs) in the ZnO grains. In the Sb_2O_3 - and SnO_2 -doped samples IBs are present in most of the ZnO grains [15, 23], and in TiO_2 -doped samples IBs are present only in some, regularly exaggeratedly grown grains [18, 24].

Based on studies of the microstructure development in ZnO ceramics doped with Bi_2O_3 and SnO_2 we realized that inversion boundaries (IBs) have a major influence on the grain growth of ZnO, while the influence of the spinel phase is subordinate to the role of IBs [25]. We proposed an inversion-boundary-induced grain-growth mechanism. At temperatures below those for the formation of the spinel phase, in the early stage of sintering, IBs nucleate in some of the ZnO grains. The ZnO grains with an IB, i.e., nuclei, anisotropically and exaggeratedly grow in the direction of the adopted defect (IB) until they collide with each other, and finally prevail in the microstructure. The results showed that the amount of IBs-triggering dopant (Sb_2O_3) influences the number of nuclei, which indeed results in either a coarse-grained microstructure for a small number of nuclei or a fine-

grained ZnO ceramic for a larger number of nuclei that are formed in the early stage of the sintering. Higher concentrations of Sb_2O_3 resulted in a fine-grained microstructure, while at lower additions of the dopant, coarse-grained ceramics were obtained with the ZnO grain size much larger than in undoped ZnO [26,27]. For the first time a coarse-grained microstructure was obtained in Sb_2O_3 -doped ZnO ceramics. This completely contradicted the general understanding of grain growth in ZnO ceramics doped with Sb_2O_3 and showed that grain growth is primarily controlled by the inversion boundaries, while the influence of the spinel phase is subordinated.

The preparation of varistor ceramics, in accordance with the classical understanding of grain-growth hindering, required larger additions of Sb_2O_3 for effective grain growth inhibition by the increased amount of the $\text{Zn}_7\text{Sb}_2\text{O}_{12}$ spinel phase at the grain boundaries. Hence, to ensure sufficient amounts of Co, Mn and Ni for doping the ZnO grains and their high conductivity, larger amounts of these dopants had to be added as well to compensate for their incorporation into the spinel phase. Understanding of the true mechanism of IBs-induced grain growth that actually controls the grain growth in the ZnO ceramics doped with IBs-triggering dopants opened a new paradigm for tailoring the microstructure and I-U characteristics of the varistor ceramics for all breakdown voltages (low, medium and high) only with the Sb_2O_3 , at much lower amounts of Sb_2O_3 and with a significantly reduced total amount of varistor dopants added to the ZnO. While in Sb_2O_3 -doped ZnO only the $\text{Zn}_7\text{Sb}_2\text{O}_{12}$ spinel phase is formed, the phase equilibria of the ZnO- Bi_2O_3 - Sb_2O_3 system, which defines the chemistry in the fully doped varistor ceramics, is much more complex and influenced by the $\text{Sb}_2\text{O}_3/\text{Bi}_2\text{O}_3$ ratio and the reactions of the $\text{Bi}_3\text{Zn}_2\text{Sb}_3\text{O}_{14}$ pyrochlore phase. In further work we determined the key compositional parameters that influence the IBs-induced grain-growth mechanism for tailoring the microstructure in ZnO ceramics doped with Bi_2O_3 and Sb_2O_3 [28]. We succeeded in preparing ZnO ceramics doped with small amounts of Bi_2O_3 and Sb_2O_3 with the microstructures ranging from coarse to fine grained. Afterwards, we were strongly encouraged that the IBs-induced grain growth mechanism could also be successfully used for tailoring the microstructure of fully doped ZnO-based varistor ceramics.

In this work the possibilities to tailor, under the influence of IBs, the microstructure and I-U characteristics of ZnO-based varistor ceramics for a significantly reduced amount of varistor dopants added to the ZnO was investigated. The samples of the varistor ceramics with the addition of only about 3 wt.% of varistor dopants were prepared by a classical ceram-

ic procedure and sintered at 1200°C . The microstructural and I-U characterisations of the samples fully confirmed that varistor ceramics with minimum amounts of secondary phases at the grain boundaries having excellent I-U characteristics in a broad range of breakdown voltages can be successfully prepared. In this way the primary role of the IBs-induced grain-growth mechanism in controlling the microstructure development in ZnO-based varistor ceramics was clearly demonstrated as well.

EXPERIMENTAL

The samples of varistor ceramics with varying compositions for the Sb_2O_3 -to- Bi_2O_3 ratio (Sb/Bi) at the same amount of Bi_2O_3 were prepared using reagent-grade powders of the ZnO and the varistor dopants Bi_2O_3 , Sb_2O_3 , Co_3O_4 , Mn_3O_4 , NiO and Cr_2O_3 . Stable water suspensions with a solids load of about 60% of the powder mixture composed of ZnO with the addition of about 3 wt.% of varistor dopants were prepared and dried on a spray drier to obtain granulates. These granulates were pressed at a pressure of 150MPa into discs with a diameter of 10 mm and a height of about 1.5 mm. The samples were sintered in a chamber furnace at 1200°C for 2 hours in an air atmosphere. The microstructures of the samples were prepared by grinding and polishing the sample pellet in a cross-sectional direction. Half of each microstructure was etched with dilute hydrochloric acid. The microstructures were analyzed on a scanning electron microscope (SEM) JEOL JSM-5800. Several SEM/BE images per sample were used for a stereological analysis of the ZnO grain size and the grain size distribution. The surface of each grain was measured and its size was calculated in terms of a diameter for circular geometry; the average ZnO grain size and the size distribution were determined from measurements of 200 to 500 grains per sample. The details are given in references 27 and 28. For the DC current-voltage (I-U) characterization, silver electrodes were painted on both parallel surfaces of the discs and fired at 600°C . The nominal varistor voltages (U_N) at $1\text{mA}/\text{cm}^2$ and $10\text{mA}/\text{cm}^2$ were measured using a Keithley 2410 Digital SourceMeter and the threshold voltage U_T (V/mm) and the non-linear coefficient α were determined. The leakage current (I_L) was measured at $0.75V_N$ ($1\text{mA}/\text{cm}^2$).

RESULTS AND DISCUSSION

The microstructures of the varistor samples with compositions V1 (Sb/Bi > 1) and V3 (Sb/Bi < 1) are presented in fig. 4. They show typical microstructures of the low doped varistor ceramics prepared in this study with minimum amounts of secondary phases,

the Bi_2O_3 phase and the $\text{Zn}_7\text{Sb}_2\text{O}_{12}$ spinel phase. The spinel phase is evidently present only in the samples with the ratio $\text{Sb}/\text{Bi} > 1$. It is fine grained with the grain size around $1 \mu\text{m}$ and homogeneously distributed at the grain boundaries of the ZnO and often also inside the ZnO grains. This last feature indicates that

they are easily overgrown and that such fine spinel particles after all do not represent serious hindering to the grain-boundary mobility and grain growth. At lower additions of Sb_2O_3 , in the samples with the ratio $\text{Sb}/\text{Bi} < 1$, the spinel phase is hardly detected and is present only in traces.

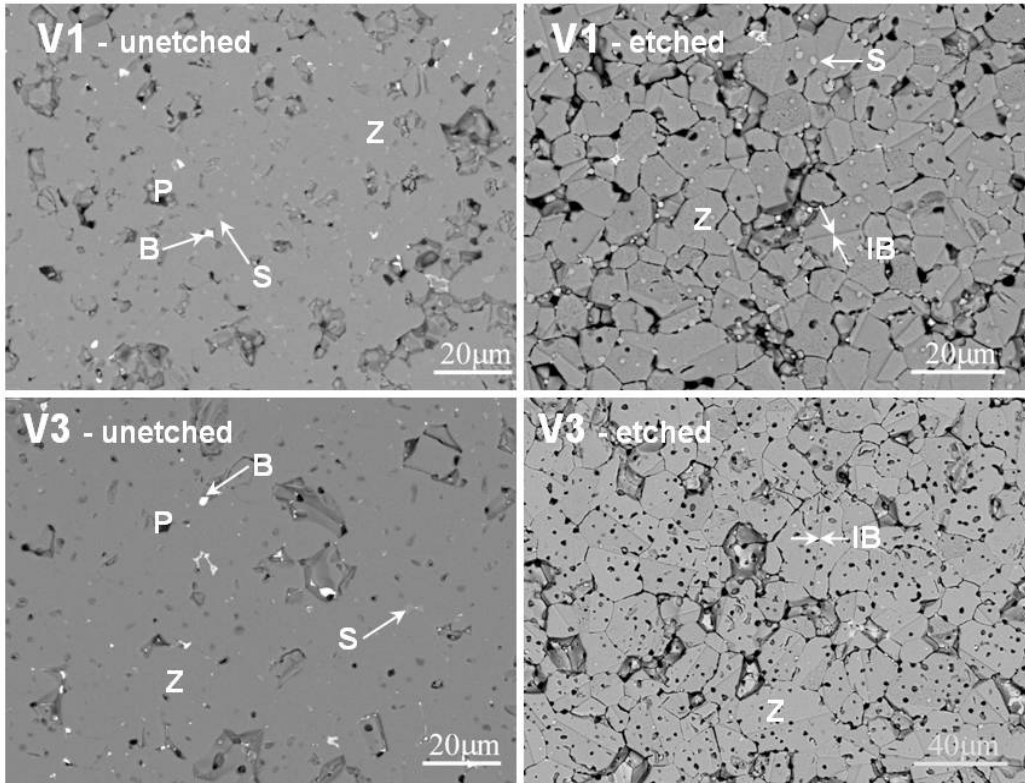


Fig 4: Backscattered electron (BE) images from scanning electron microscope (SEM) of the varistor samples V1 and V3, sintered at 1200°C for 2 hours. Z: ZnO phase; B: Bi_2O_3 -rich phase, S: $\text{Zn}_7\text{Sb}_2\text{O}_{12}$ spinel phase, IB: inversion boundary; P: pore.

However, regardless of the amount of added Sb_2O_3 and the ratio Sb/Bi , in all the samples, as can be seen from their microstructures, the inversion boundaries (IBs) are clearly present, in practically each ZnO grain. The results of the stereological analysis (the average ZnO grain size) of the samples are given in Table 1.

Table 1: Stereological (average ZnO grain size G) and current-voltage (I - U) characteristics (threshold voltage U_T , coefficient of nonlinearity α and leakage current I_L) of the low doped ZnO-based varistor ceramics with various compositions (V), sintered at 1200°C .

Sample	G (μm)	U_T (V/cm)	α	I_L (μA)	U_{GB} (V)
V1	7.0	3470	54	0.30	2.4
V2	11.1	2100	38	0.14	2.4
V3	14.4	1750	32	0.20	2.5
V4	21.3	1300	23	1.43	2.8

The size of the ZnO grains increased with decreasing of the Sb/Bi ratio from the sample V1 to the sample V4, from 7 to 21 μm , respectively. The observed microstructural characteristics of the samples clearly demonstrate the key role of IBs in the grain growth and microstructure development

Having in mind that the electrical characteristics of varistor ceramics are determined by the characteristics of the grain boundaries and the grains an ideal varistor ceramic would be composed only of highly conductive ZnO grains with the proper size for the required threshold voltage, separated only by highly non-linear, varistor-type grain boundaries. The microstructures as obtained in these samples of the low doped varistor ceramics are approaching this ideal. They are in striking contrast to the microstructure of the standard varistor ceramic presented in fig. 3, which contains significant amounts of secondary phases. The high microstructural homogeneity and significantly increased effective contact among

the ZnO grains could possibly also result in an enhancement of the I-U characteristics and energy absorption capability of the low doped ZnO-based varistor ceramics.

The I-U characteristics of the samples are given in Table 1. The threshold voltages U_T (breakdown voltage per unit thickness of ceramics; V/cm) of the samples are in the range from 3500V/cm to 1300 V/cm and clearly correlate with the average ZnO grain sizes, which are in the range from 7 to 21 μm , respectively. Most of the samples had excellent I-U nonlinearity with a coefficient of nonlinearity α ranging from 30 to 50, which is also demonstrated by a sharp transition from a highly resistive to a highly conductive state in the curves of the electric field (E) vs. current density (J) presented in fig. 5. The samples also have a very low leakage current I_L of about 0.2 μA . An estimation of the average breakdown voltage of the individual ZnO grain boundary U_{GB} (V) from the average ZnO grain size G and the threshold voltage U_T (V/cm) in accordance with the expressions $U_{GB} = U_T/N$ (where $N = 10000/G(\mu\text{m})$... number of grain boundaries per unit thickness) gave values in the range from 2.4V to 2.8V. Such values indicated the excellent varistor characteristics of the grain boundaries in all the samples of the low doped varistor ceramics. This can also mean that 75 to 90% of all the grain boundaries in the samples are varistor active in regard to the ideal U_{GB} , which is about 3.2V.

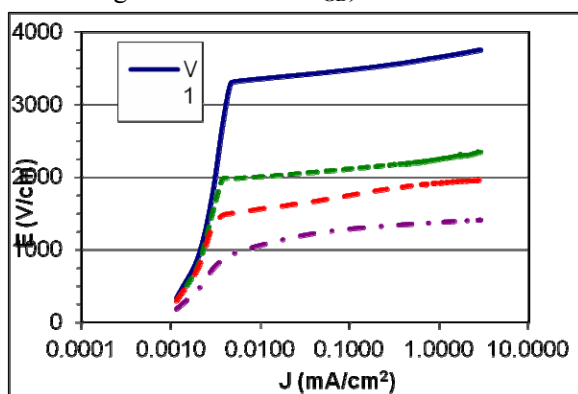


Fig. 5: Electrical field (E) vs. current density (J) of the varistor samples sintered at 1200°C.

CONCLUSIONS

In recent years we discovered that inversion boundaries (IBs) play a key role in controlling the grain growth and microstructure development in ZnO ceramics doped with Sb_2O_3 (or other dopants which form a spinel phase in the reaction with ZnO and also trigger the formation of IBs) while the role of the spinel phase is subordinated. We also demonstrated that an IBs-induced grain-growth mechanism enables tailoring of the microstructure from a coarse- to a

fine-grained one in the case of ZnO ceramics doped with Sb_2O_3 and also ZnO ceramics doped with Bi_2O_3 and Sb_2O_3 . These results strongly indicate that using the primarily role of IBs in the grain growth and microstructure development should also enable the preparation of the coarse- or fine-grained ZnO-based varistor ceramics with a broad range of breakdown voltages at significantly reduced amount of varistor dopants added to the ZnO. The prospects of these expectations were studied in this work. The samples of low doped varistor ceramics with the addition of only about 3 wt.% of varistor dopants to ZnO (typical additions are 7 to 10 wt.%) were prepared by the classical ceramic procedure and sintering at 1200°C. All the samples had a highly homogeneous microstructure with the minimum amounts of secondary phases, namely the Bi_2O_3 phase and the $\text{Zn}_7\text{Sb}_2\text{O}_{12}$ spinel phase. Subtle variations of the starting composition for the Sb_2O_3 -to- Bi_2O_3 ratio enabled tailoring of the average ZnO grain size of the sample in the range from 7 to 21 μm and hence the threshold voltages U_T in the range from 3500V/cm to 1300V/mm, respectively. All the samples had good I-U nonlinearity (coefficient of nonlinearity α from 25 to 55) and a low leakage current I_L ($< 1\mu\text{A}$).

The results fully confirmed the expectations and showed that an IBs-induced grain-growth mechanism enables tailoring the microstructure and hence I-U characteristics in broad range of voltages also in fully doped ZnO-based varistor ceramics. Varistor ceramics with excellent I-U characteristics can be prepared with compositions containing a significantly reduced amount of varistor dopants added to the ZnO. This means significant savings on raw materials and a reduction of the production costs for the varistors. The microstructure of such varistor ceramics, which contains minimum amounts of secondary phases, approaches an ideal one, composed only of highly conductive ZnO grains of suitable size for certain breakdown voltage, separated only by highly non-linear grain boundaries.

Acknowledgement The authors acknowledge the financial support by the Slovenian Research Agency (Program Contract No. P2-0084 and Project Grant L2-9175).

REFERENCES

- [1] Stevens, M., Current & Voltage Transient Protection ... Theory to Application, Measurements & Control, Measurements & Control, 1996, 178, 161-165
- [2] Skibinski, G. L., Thunes, J. D., Mehlhorn, W., Effective Utilization of Surge Protection Devices, IEEE Transactions on Industry Applications, 1986, IA-22, 641-652

- [3] Gupta, T. K., Application of zinc oxide varistors, *J. Am. Ceram. Soc.*, 1990, 73, 1817-1840
- [4] Clarke, D. R., Varistor ceramics, *J. Am. Ceram. Soc.*, 1999, 82, 485-502
- [5] Eda, E., Zinc oxide varistors, *IEEE Electrical Insulation Magazine*, 1989, 5, 28-41
- [6] Olsson, E., Dunlop, G. L., Characterization of individual interfacial barriers in a ZnO varistor material, *J. Appl. Phys.*, 1989, 66, 3666-3675
- [7] Tao, M., Bui, A., Dorlante, O., Loubiere, A., Different 'single grain junctions' within a ZnO varistor, *J. Appl. Phys.*, 1987, 61, 1562-1567
- [8] Inada, M., Crystal phases of nonohmic zinc oxide ceramics, *Jpn. J. Appl. Phys.*, 1978, 17, 1-10
- [9] Inada, M. Formation mechanism of nonohmic zinc oxide ceramics, *Jpn. J. Appl. Phys.*, 1980, 19, 409-419
- [10] Inada, M., Effect of heat-treatment on crystal phases, microstructure and electrical properties of nonohmic zinc oxide ceramics, *Jpn. J. Appl. Phys.*, 1979, 18, 1439-1446
- [11] Wong, J., Sintering and varistor characteristics of ZnO - Bi₂O₃ ceramics, *J. Appl. Phys.*, 1980, 51, 4453-4459
- [12] Senda, T., Bradt, R. C., Grain growth in sintered ZnO and ZnO-Bi₂O₃ ceramics, *J. Am. Ceram. Soc.*, 1990, 73, 106-114
- [13] Dey, D., Bradt, R. C., Grain growth of ZnO during Bi₂O₃ liquid-phase sintering, *J. Am. Ceram. Soc.*, 1992, 75, 2529-2534
- [14] Kim, J., Kimura, T., Yamaguchi, T., Microstructure development in Sb₂O₃-doped ZnO, *J. Mater. Sci.*, 1989, 24, 2581-2586
- [15] Senda, T., Bradt, R. C., Grain growth in zinc oxide during the sintering of zinc oxide-antimony oxide ceramics, *J. Am. Ceram. Soc.*, 1991, 74, 1296-1302
- [16] Ito, M., Tanahashi, M., Uehara, M., Iga, A., The Sb₂O₃ addition effect on sintering ZnO and ZnO+Bi₂O₃, *Jpn. J. Appl. Phys.*, 1997, 36, L1460-L1463
- [17] Suzuki, H., Bradt, R. C., Grain Growth of ZnO in ZnO-Bi₂O₃ Ceramics doped with TiO₂ addition, *J. Am. Ceram. Soc.*, 1995, 78, 1354-1360
- [18] Makovec, D., Kolar, D., Trontelj, M., Sintering and Microstructural development of Metal Oxide Varistor Ceramics, *Mat. Res. Bull.*, 1993, 28, 803-811
- [19] Nunes, S. I., Bradt, R. C., Grain Growth in ZnO and ZnO-Bi₂O₃ Ceramics with Al₂O₃ additions, *J. Am. Ceram. Soc.*, 1995, 78, 2469-2475
- [20] Han, J., Mantas, P. Q., Senos, A. M. R., Densification and grain growth of Al-doped ZnO, *J. Mater. Res.*, 2001, 16, 459-468
- [21] Tanahashi, M., Ito, M., Murao, M., Iga, A., Effect of Al-doping on the grain growth of ZnO, *Jpn. J. Appl. Phys.*, 1997, 36, L573-L576
- [22] Bernik, S., Daneu, N., Characteristics of ZnO-based varistor ceramics doped with Al₂O₃, *J. Europ. Ceram. Soc.*, 2007, 27, 3161-3170
- [23] Bernik, S., Daneu, N., Characteristics of SnO₂-doped ZnO-based varistor ceramics, *J. Eur. Ceram. Soc.*, 2001, 21, 1879-1882
- [24] Bernik, S., Daneu, N., Rečnik, A., Inversion boundary induced grain growth in TiO₂ or Sb₂O₃ doped ZnO-based varistor ceramics, *J. Eur. Ceram. Soc.*, 2004, 24, 3703-3708
- [25] Daneu, N., Rečnik, A., Bernik, S., Kolar, D., Microstructural Development in SnO₂-Doped ZnO-Bi₂O₃ Ceramics, *J. Am. Ceram. Soc.*, 2000, 83, 3165-3171
- [26] Daneu, N., Rečnik, A., Bernik, S., Grain Growth Control in Sb₂O₃-Doped Zinc Oxide, *J. Am. Ceram. Soc.*, 2003, 86, 1379-1384
- [27] Bernik, S., Bernard, J., Daneu, N., Rečnik, A., Microstructure development in Low-Antimony-Doped Zinc Oxide Ceramics, *J. Am. Ceram. Soc.*, 2007, 90, 3239-3247
- [28] Bernik, S., Podlogar, M., Daneu, N., Rečnik, A., Grain-growth phenomena in ZnO-based ceramic, *Mat. Sci. Forum*, 2007, 558-559, 857-862